



## Investigation on the Effect of Atmosphere on the Pores of Sintered Astaloy CrM Steel

M. Makarem <sup>a</sup>, M. Haddad Sabzevar <sup>a</sup>, A. Haerian Ardakani <sup>\*b</sup>

<sup>a</sup> Department of Materials Science Engineering, Ferdowsi University of Mashhad, Mashhad, Iran

<sup>b</sup> Sadjad Institute of Higher Education, Mashhad, Iran

### PAPER INFO

#### Paper history:

Received 29 February 2012

Accepted in revised form 24 January 2013

#### Keywords:

Image Analyses

Powder Metals

Sintering Process

Sintering Atmosphere

Pores Morphology

### ABSTRACT

Image analysis is used to study the effect of sintering atmosphere and sintering time on the pores morphology of Astaloy CrM. The pores morphology was described by means of some parameters, Circular Diameter ( $D_c$ ) - which shows the diameter of equivalent circle for comparing the pore size,  $F_{\text{Elongation}}$  and  $F_{\text{Shape}}$  - which have different geometrical meanings. The results were interpreted with reference to an elliptical geometry which represents the theoretical shape to which pores tend. Effect of different sintering atmospheres ( $N_2$ , Cracked Ammonia ( $NH_3$ ), Ar, Vacuum and air) at  $1200^\circ C$  was investigated. The results showed 20% decrease of maximum  $D_c$  in vacuum and cracked ammonia in comparison with other atmospheres. The pore size measurement by image analyses confirmed the variation of density measured by Archimedes method.  $D_c$  was affected by atmosphere more than  $F_{\text{Shape}}$  and  $F_{\text{Elongation}}$ . Furthermore,  $F_{\text{Shape}}$  was more sensitive than  $F_{\text{Elongation}}$  to different sintering atmospheres. Mechanical properties of specimens have a significant relation with percentage of pores (porosity) and morphology. Vacuum atmosphere led to more spherical and finer pores. Sintering atmosphere has significant effect on pores size and pore distribution in comparison with other morphological parameters in Astaloy CrM. Differences in  $F_{\text{Shape}}$  and  $F_{\text{Elongation}}$  factors are more observable in large pores (over  $75\mu m^2$  area) in comparison with smaller ones.  $F_{\text{Shape}}$  seems to be more suitable than  $F_{\text{Elongation}}$  for evaluating the effect of sintering variables on the evolution of pores morphology.

doi: 10.5829/idosi.ije.2013.26.07a.07

## 1. INTRODUCTION

In this study, image analysis is used to study the effect of the sintering atmosphere on porosity characteristics of Astalloy CrM. Bonding of metallic or ceramic powder particles takes place in solid phase, or in some cases, in the presence of a partially melted phase at sintering temperature. In the early stages of sintering particles join at their interfaces by forming necks. Later, the necks grow continually during further stages of sintering, changing the morphology and volume fraction of pores continuously till the end of the sintering process. Therefore, morphology and density of a metallic or ceramic material can be controlled by varying the sintering process parameters [1].

Structural changes related to neck growth during sintering is dependent on mass transfer mechanisms

which are mainly diffusion-based processes [1, 2]. Diffusion is a heat-activated process, meaning that atoms require heat energy for their movements. There are several parameters affecting the end results of sintering, one of the most important ones being the sintering atmosphere. Sintering atmosphere is chosen so as to inhibit oxidation of powder particles during sintering, and hence it varies with the material that is being sintered [2]. An appropriate atmosphere is the one which helps to decrease active pore surface area by rounding the pores, increase the number and strength of metallic bonds between particles, increase density, decrease porosity, homogenize the structure and reduce defects [3].

Presence of pores in sintered material reduces its mechanical properties by reducing the load bearing cross section and causing local stress accumulation, so that they act as sites for crack nucleation. Amongst various mechanical properties, fatigue behavior of the

\*Corresponding Author Email: [a\\_haerian@sadjad.ac.ir](mailto:a_haerian@sadjad.ac.ir) (A. Haerian Ardakani)

material is most sensitive to porosity and pore morphology [3, 4].

The pores are sites for crack initiation and best location for crack propagation as well. Moreover, they constitute a favorable path for crack propagation. Porosity affects mechanical properties through geometry and distribution of pores in the PM part. Geometrical parameters affecting fatigue resistance of the material include shape, size and roundness, the degree of interconnection, volume fraction and statistical distribution of pores [4].

## 2. MATERIALS AND METHODS

Material used for this research was pre-alloyed Astaloy CrM powder having nominal composition: Fe, 3% Cr, 0.5% Mo. To this pre-alloyed powder, 0.3% graphite and 0.8% wax were added as lubricant. The test specimens were pressed at room temperature and 600MPa. The pressed parts were then sintered for 45 min at 1200°C under different atmospheres as shown in Table 1 in a laboratory tube furnace. Three samples for each combination of test parameters were prepared for further studies. Reference samples were sintered in air.

In quantitative description of planar shapes, two dimensional shape parameters are used to compare the features of pores in powder metallurgy (PM) products. This method is called fingerprinting by Fishmeister. This terminology, if properly applied, provides accurate information on three-dimensional shapes.

Here, the number, length, and surface area of pores are measured to get a general overview of statistical scatter of pores in three dimensions [5]. In order to prepare all the metallographical samples under similar conditions, all the samples were mounted together and further treated for metallographic tests by standard methods [5]. Careful metallographic preparation is particularly important for the analysis of sintered structures, because the shape of pores is as important to strength as their quantity. When the specimen is properly prepared, the areal fraction of porosity will equal to its volume fraction, and these must be equal to the porosity calculated by actual measurement of density of porous material and pore-free density of a uniformly dense part by Equation (1):

$$V_p = (P_d - M_d)/P_d \quad (1)$$

here,  $V_p$  is the volume fraction of pores as calculated,  $P_d$  is theoretical density of the powder (density of the material without pores), and  $M_d$  is the actual density of PM samples [6].

Quantitative parameters were measured using Clemex Image Analysis and the PM package of MIP software produced by Nahamin Pardazane Asia Co. The results from the two sources were compared.

Theoretical density of Astaloy CrM was taken as 7.80 g/cm<sup>3</sup>. Densities of as-sintered samples were determined by Archimedes method. Density calculated using volume fraction of pores obtained from the two image processing techniques was cross checked by that determined by Archimedes method.

The following geometrical parameters were used for determination of pore morphology:

- ❖  $D_{circle}$  = diameter of the equivalent circle with surface area equal to that of the pore as seen in the micrograph.
- ❖  $A$  = the surface area of pore.
- ❖  $f_{elong}$  = elongation factor which is the ratio  $D_{min}/D_{max}$ .  $D_{max}$  being the largest diameter, and  $D_{min}$  the smallest diameter of the pore measured on the micrograph (see Figure 1).
- ❖  $f_{shape}$  = shape factor which is a measure of roundness of pore.  $f_{shape} = 4\pi A/P^2$ , where  $A$ =surface area, and  $P$ =perimeter of the pore.

$$f_{elong} = D_{min}/D_{max} \quad (2)$$

$$f_{shape} = 4\pi A/P^2 \quad (3)$$

Both elongation factor and shape factor are in the range 0 to 1. Shape factor is affected by surface roughness and ratio of periphery to area of the pore. For a circle, it equals 1, and for other shapes is as shown in Figure 2a. The closer this factor to 1, the smoother and more spherical is the pore [6]. Elongation factor is an indication of the difference between longest and shortest dimension of the pore. The closer to 0, the more elongated is the pore (Figure 2b). Variation of elongation and shape factors with pore geometry is shown in Figures 3 and 4. Since in general larger pores are more irregular, the pores were divided into two categories, namely: small pores with surface area under 75 square microns, and large pores with surface area over 75 square microns as proposed by other researchers [7]. Quantitative parameters were measured by image analyzer software. After calibration of the software, 10 random surfaces of each sample were analyzed. In total, over 6000 pores were studied and measured. The results were double checked by qualitative analysis of SEM micrographs. Mechanical properties were measured on 4 tension test specimens of each sample. Tension tests were carried out on 700KN Zwick testing machine.

TABLE 1. Sintering atmospheres

	Sintering Temperature (°C)	Sintering Time (min)	Sintering Atmosphere
1	1200	45	Cracked ammonia (25% N <sub>2</sub> , 75% H <sub>2</sub> )
2	1200	45	Pure nitrogen (100% N <sub>2</sub> )
3	1200	45	Argon
4	1200	45	Vacuum

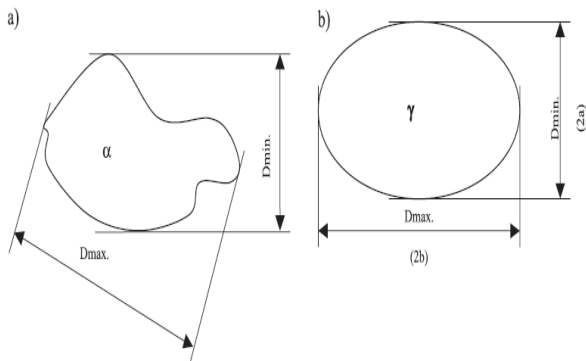


Figure 1. Feret diameters of: (a) a pore, and (b) the equivalent ellipse

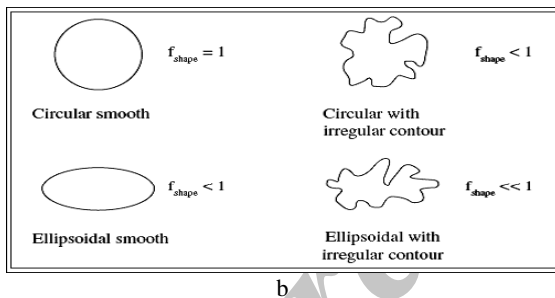
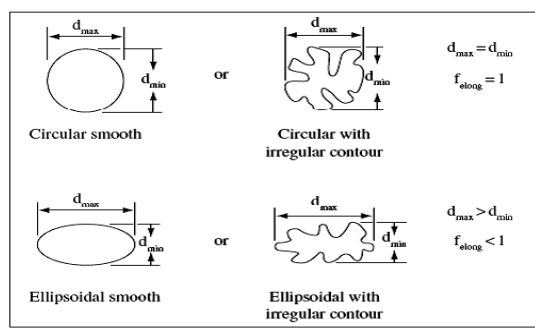


Figure 2. Values of a)  $F_{shape}$ ; and b)  $F_{elong}$  for different pore geometries

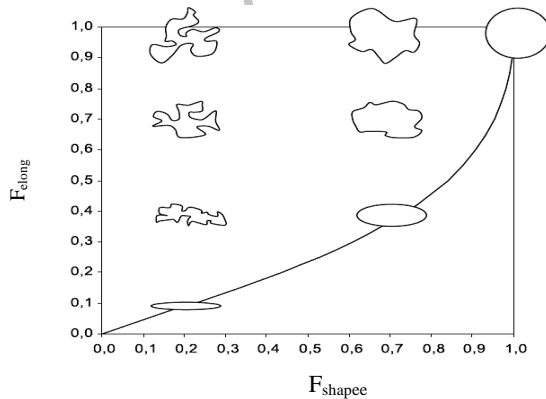


Figure 3. Variation of elongation and shape factors with pore geometry [6]

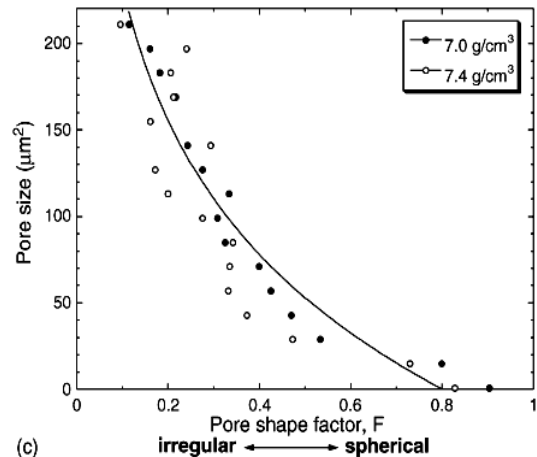


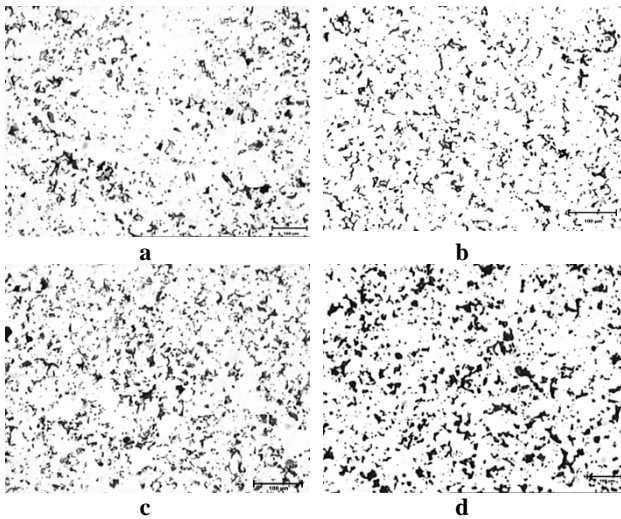
Figure 4. Variation of elongation and shape factors with pore size [8]

TABLE 2. Pore measurements for samples sintered in different atmospheres

Group	Sintering atmosphere	Final density (g/cm <sup>3</sup> )	Pore fraction (%)		Total number of pores
			Theoretical	Image analysis	
1	Vacuum	7.23	7.3	7.2±0.15	6818
2	Cracked Ammonia	7.21	7.5	7.4±0.2	6582
3	N <sub>2</sub>	7.10	8.9	8.3±0.5	7204
4	Argon	7.04	9.7	9.9±0.7	9374

### 3. RESULTS AND DISCUSSION

Pore morphology of samples in four test atmospheres are shown in Figure 5. The SEM micrographs at two different magnifications are presented in Figure 6. Density and pore fraction of samples were determined by image analysis and calculated by Archimedes's rule. These results for all four classes of materials are presented in Table 2. Figure 7 shows the pore size distribution for both sizes, i.e. smaller and larger than 75 square micron pores. The figure shows that for small pores the largest diameter of the equivalent circle for groups 1 and 2 are 10% and 25% smaller than that for groups 3 and 4, respectively. However, the results for larger pores (larger than 75 square microns) seem to be more uniform for all four groups (Figure 7 b). Figure 8 shows the largest equivalent circle diameter for the four groups of samples.



**Figure 5.** Pore morphology of samples sintered under: a) Vacuum, b) NH<sub>3</sub>, c) Nitrogen, d) Argon

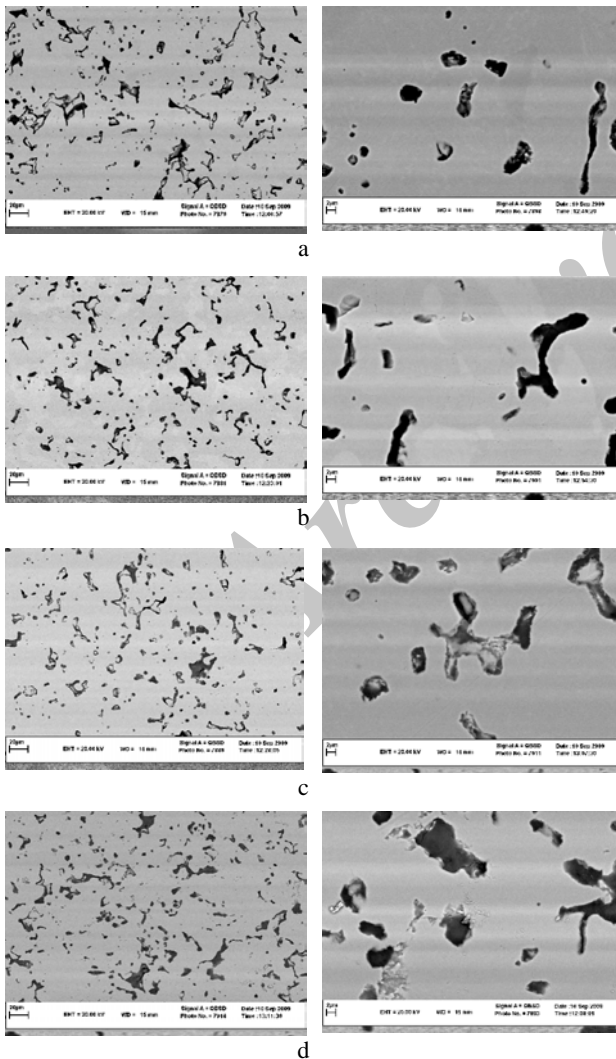


**Figure 6.** SEM micrographs of samples sintered under a) Vacuum, b) NH<sub>3</sub>, c) Nitrogen, d) Argon

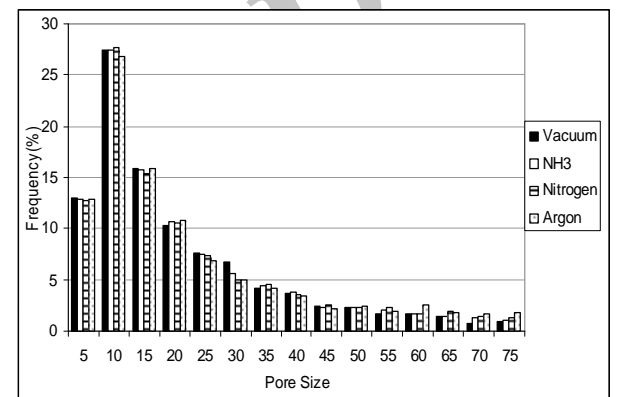
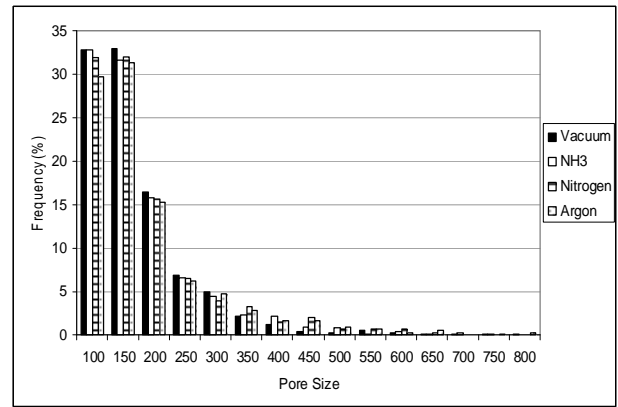


**Figure 7.** Pore size distribution for four groups of samples: a) large pores (larger than 75 square microns), and b) small pores (smaller than 75 square microns)

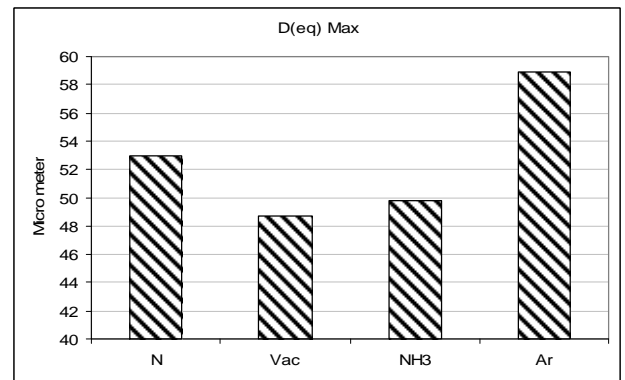
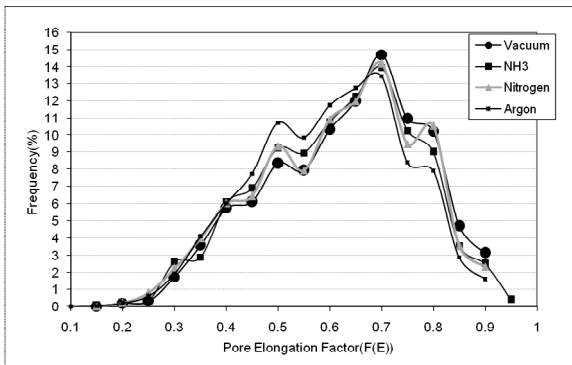
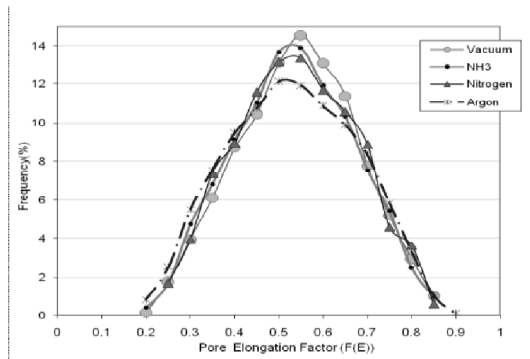


**Figure 8.** Largest diameter of equivalent circle for four groups of samples, (i.e. samples sintered under: a) Vacuum, b) NH<sub>3</sub>, c) Nitrogen, and d) Argon)

Comparing the elongation factor for both size range of pores shows that samples sintered under vacuum and cracked ammonia give smaller and rounder pores as compared to the other two atmospheres (Figure 9).

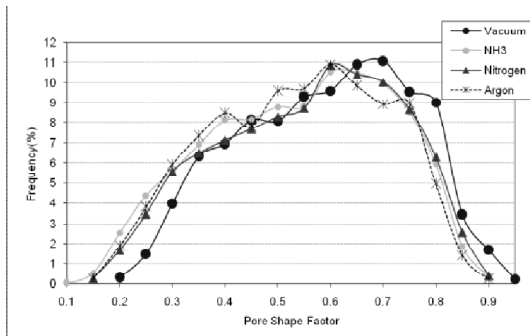


a

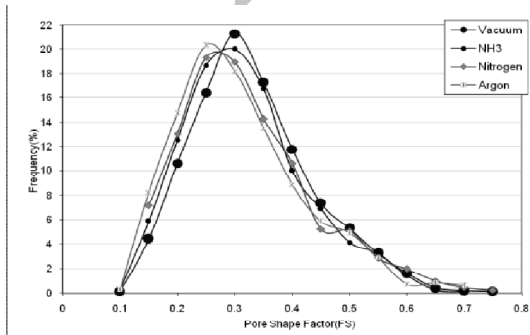


b

**Figure 9.** Elongation factor distribution for: a) pores smaller than 75 square microns and b) pores larger than 75 square microns



a

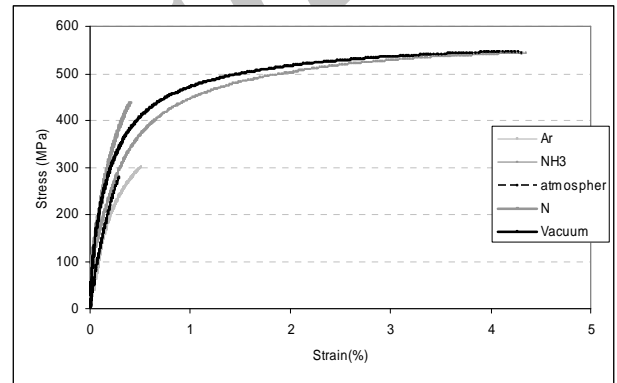


b

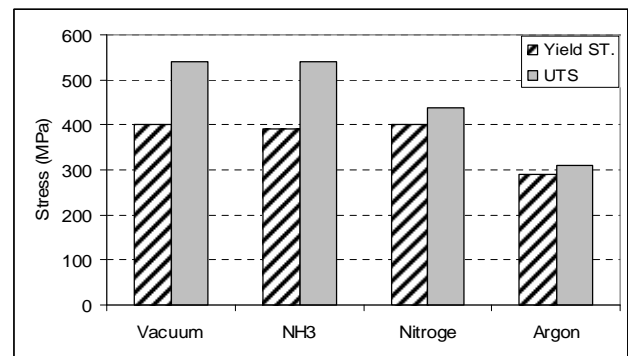
**Figure 10.** Shape factor distribution for: a) pores smaller than 75 square microns and b) pores larger than 75 square microns

Figure 10b as compared to smaller pores (Figure 10a) shows that the shape factor ( $F_{shape}$ ) for larger pores tend to smaller values. At the same time, both figures show that this factor is highest for samples sintered under vacuum, followed by cracked ammonia, and nitrogen and is smallest for samples sintered under Argon. However, the distribution of  $F_{shape}$  for all samples is almost the same. This indicates that the pore shape changes from more roundish periphery to irregular one. This change is more pronounced for smaller pores (Figure 10a).

Tensile test results (Table 3) indicate higher UTS,  $\sigma_y$  and percent elongation for samples sintered under vacuum and cracked ammonia as compared to the other two atmospheres (Figures 11 and 12).



**Figure 11.** Stress-strain curves of samples



**Figure 12.** UTS and  $\sigma_y$  for four groups of samples

**TABLE 3.** UTS and  $\sigma_y$  and elongation for four groups of samples

	$\sigma_y$ (MPa)	UTS (MPa)	Elongation (%)
<b>Vacuum</b>	400±11	540±15	4.3±0.1
<b>NH<sub>3</sub></b>	390±12	540±14	4.35±0.13
<b>Nitrogen</b>	400±18	437±10	0.39±0.06
<b>Argon</b>	290±10	310±12	0.52±0.07

#### 4. CONCLUSIONS

1. Density measurements and quantitative evaluation of pore parameters showed that pore morphology in sintered parts made of prealloyed Astaloy CrM changes with sintering atmosphere. These changes take place at different rates.
2. Vacuum and cracked ammonia atmospheres render more or less similar morphologies, with smaller and rounder pores which give better end results especially for mechanical properties. Although volume fraction of pores in cracked ammonia and nitrogen are different, shape factor and elongation factor for these two groups are similar for small pores.
3. In general, vacuum and cracked ammonia are better atmospheres for sintering of Astaloy CrM powder.
4. Since pore length has significant effect on dynamic properties of sintered material, measuring this parameter is helpful in predicting dynamic behavior of the material.
5. Pore size is much more significantly affected by sintering atmosphere than other morphological parameters. Crack initiation in fatigue loading is restricted to very few large irregular pores. All efforts to correlate average pore sizes or shape factors with fatigue strength values yield at best tendencies. If only the largest pores are taken into account, quantitative relations can be established which open the route to better service performance.
6. Change of atmosphere affects the largest pores more severely than any other parameter.

#### 5. ACKNOWLEDGEMENTS

The authors are grateful to Mr. Abbasi and the personnel of Khorasan Powder Metallurgy Company (KPM) and Dr. Arvand and the personnel of Mashhad Powder Metallurgy Company (MPM) for their great contributions and support. Also grateful to Nahamin Pardazan Asia Co. for the contribution they made to use their image analysis software (MIP).

#### 6. REFERENCES

1. "Handbook, asm", *Powder Metal Technologies and Applications*, Vol. 7, (1998).
2. Kang, S.-J. L., "Sintering: Densification, grain growth and microstructure", *Butterworth-Heinemann*, (2004).
3. Marcu Puscas, T., Signorini, M., Molinari, A. and Straffelini, G., "Image analysis investigation of the effect of the process variables on the porosity of sintered chromium steels", *Materials characterization*, Vol. 50, No. 1, (2003), 1-10.
4. Beiss, P. and Dalgic, M., "Effect of pore structure on bending fatigue strength of sintered steel", *Advances in Powder Metallurgy and Particulate Materials*, Vol. 4, (1996), 13-21
5. Vander Voort, G. F., "Asm handbook: Metallography and microstructures", *ASM International (OH)*, (2004).
6. Pavanati, H. C., Maliska, A. M., Klein, A. N. and Muzart, J. L. R., "Comparative study of porosity and pores morphology of unalloyed iron sintered in furnace and plasma reactor", *Materials Research*, Vol. 10, No. 1, (2007), 87-93.
7. Chawla, N. and Deng, X., "Microstructure and mechanical behavior of porous sintered steels", *Materials Science and Engineering: A*, Vol. 390, No. 1, (2005), 98-112.
8. Hoganas, A., "Hoganas handbook for sintered components", *Material and Powder Properties*, (1997).

## Investigation of the Effect of Atmosphere on the Pores of Sintered Astaloy CrM Steel

M. Makarem <sup>a</sup>, M. Haddad Sabzevar <sup>a</sup>, A. Haerian Ardakani <sup>b</sup>

<sup>a</sup> Department of Materials Science Engineering, Ferdowsi University of Mashhad, Mashhad, Iran

<sup>b</sup> Sadjad Institute of Higher Education, Mashhad, Iran

### PAPER INFO

### چکیده

#### Paper history:

Received 29 February 2012

Accepted in revised form 24 January 2013

#### Keywords:

Image Analyses

Powder Metals

Sintering Process

Sintering Atmosphere

Pores Morphology

برای مطالعه‌ی مورفولوژی حفرات در نمونه‌های تف‌جوشی شده از پودر Astaloy CrM از پردازش تصویر استفاده شد. بدین منظور و برای توصیف مورفولوژی حفرات دو پارامتر فاکتور شکل ( $f_{shape}$ ) و فاکتور کشیدگی ( $f_{elong}$ ) تعریف شد. این دو فاکتور شکل هندسی حفرات و میزان کشیدگی آن‌ها را بیان می‌کنند. از طرفی، با تعریف (DC) به عنوان قطر دایره‌ی معادل حفرات اندازه‌ی آنها تعیین شد. تف‌جوشی در دمای ۱۲۰۰ درجه‌ی سانتی‌گراد و در چهار اتمسفر آمونیاک شکسته، آرگون، نیتروژن و خلا انجام گرفت. پس از آماده‌سازی نمونه‌ها و تهیه تصاویر به کمک میکروسکوپ نوری از سطوح مختلف به کمک پارامترهای تعریف شده مورفولوژی حفرات ارزیابی و مقایسه شدند. بررسی‌ها نشان از کاهش ۲۰ درصدی قطر دایره‌ی معادل ماکزیمم در نمونه‌های تف‌جوشی شده در خلا و آمونیاک شکسته نسبت به دیگر نمونه‌ها داشت. همچنین، کاهش درصد حفرات در این دو اتمسفر نشان از بالاتر بودن چگالی دو نمونه‌ی تف‌جوشی شده نسبت به اتمسفرهای آرگون و نیتروژن دارد. با مطالعه‌ی نتایج کمی  $f_{elong}$  و  $f_{shape}$  در نمونه‌های تف‌جوشی شده و مقایسه‌ی آنها تاثیر قابل توجه اتمسفر تف‌جوشی بر  $f_{shape}$  (فاکتور شکل) حفرات نسبت به  $f_{elong}$  مشاهده شد. این اختلاف نشان از تاثیر بیشتر اتمسفر تف‌جوشی بر تغییر شکل حفرات نسبت به هندسه آنها دارد. از طرفی، نتایج بررسی نشان از اهمیت اتمسفر تف‌جوشی بر روی اندازه‌ی حفرات در مقایسه با  $f_{shape}$  (فاکتور شکل) داشت. نمونه‌های تف‌جوشی شده در اتمسفر خلا و آمونیاک دارای حفراتی کوچک‌تر و فاکتور شکل نزدیک‌تر به یک را نشان داد. نتایج حاصل از آزمون‌های کشش و اندازه‌گیری چگالی مشاهدات انجام شده را تایید نمود.

doi: 10.5829/idosi.ije.2013.26.07a.07